NETWORKS AND HETEROGENEOUS MEDIA
©American Institute of Mathematical Sciences
Volume **2**, Number **4**, December **2007**

Website: http://aimSciences.org

pp. **647–660**

SPATIAL INSTABILITIES AND SIZE LIMITATIONS OF FLOCKS

J. J. P. Veerman

Department of Mathematics and Statistics
Portland State University, Portland, OR 97207, USA
and Departamento de Matemática Aplicada
Universidad de Granada, Granada, 18071, Spain

B. D. Stošić

Departamento de Estatística e Informática
Universidade Federal Rural de Pernambuco
Rua Dom Manoel de Medeiros s/n, Dois Irmãos
52171-900 Recife-PE, Brasil

A. Olvera

Departamento de Matemáticas y Mecánica, IIMAS
Universidad Nacional Autónoma de México
Apdo. Postal 20-726, México D.F. 04510, México

Abstract. The movement of flocks with a single leader (and a directed path from it to every agent) can be stabilized over time as has been shown before (for details see [3] and prior references therein, shorter descriptions are given in [1, 4]). But for large flocks perturbations in the movement of the leader may nonetheless grow to a considerable size as they propagate throughout the flock and before they die out over time. We calculate the effect of this "finite size resonance" in two simple cases, and indicate two applications of these ideas. The first is that if perturbations grow as the size of the flock gets larger, then the size of the flock will have a natural limitation. Our examples suggest that for flocks with a *symmetric* communication graph perturbations tend to grow much slower than in the *asymmetric case*. The second application concerns a simple traffic-like problem. Suppose the leader accelerates from standstill to a given velocity and a large flock is supposed to follow it. The acceleration of the leader is the 'perturbation'.

1. **Introduction.** Over the past decade, systems of coupled linear differential equations have been receiving increased attention in the context of modeling collective behavior of groups of agents with limited interaction range, such as flocks, herds (see references in [3]), urban traffic. Typically, it is assumed that a single agent "sees" the other agents only up to a limited range, and while individual equations of motion are rather trivial, collective behavior of large groups is capable of reproducing a wide spectrum of diverse, realistic phenomena, such as stop and go traffic, one dimension lattices and density wave propagation.

The movement of flocks with a leader can be stabilized over time as has been shown before (for details see [3] and prior references therein, shorter descriptions are given in [1, 4]). But for large flocks perturbations in the movement of the

2000 *Mathematics Subject Classification.* Primary: 34D05, 39A11; Secondary: 93B60, 92B05.
Key words and phrases. dynamics of flocks, spatial instabilities.

leader may nonetheless grow to a considerable size as they propagate throughout the flock and before they die out over time. If this happens, the size of the flock will have a natural limitation. This limitation depends of course on the size of common perturbations, the maximum allowable distance between members of flock — especially between those farthest removed from the leader — and the spatial rate with which the perturbation gets amplified. The first two depend largely on biological input. We study the latter by means of modeling the situation with ordinary differential equations, theoretically as well as numerically.

These equations are coupled, because each agent adjusts its acceleration according to the position and velocity of certain neighbors it is allowed to sense. Thus the behavior of the system as a whole will depend to a large extent on the directed graph (the *communication graph*, see [3] for a detailed description) that encodes the information as to which agent senses which others. To gain a deeper conceptual understanding of the phenomena involved we limit ourselves to flocks moving on the real line with linear equations of motion. Of course our study applies equally well to any physical system satisfying a linear equation of motion that involves many fewer neighbors than the size of the system (such as particles on a one dimensional lattice connected by springs, or traffic in a single lane).

Mathematically these ideas are of interest, because it turns out that global behavior is crucially dependent on the communication graph. As we show below, there are some cases in which the amplitude grows exponentially in the size of the flock, whereas in others the growth is only linear. In the former case a large eigenvalue causes the system to be spatially unstable at an *exponential* rate. In the latter, a curious small divisor problem occurs for large but finite flocks. (We use the term "finite size resonance" for this effect.) Since this is nonetheless a much more stable situation — the amplitude of the perturbation grows only *linearly* in the size of the flock — it seems a good reason for flocking animals to prefer this kind of communication graph over the other (not to mention possible applications in traffic-like situations).

This small divisor problem is (surprisingly) present already in an extremely simple setup, and this may help in shedding light on collective agent behavior in a number of more complex situations (similar phenomena occur in more complicated models, as is evidenced by numerical experiments.) More precisely, we study a system of coupled linear differential equations, where each agent reacts only to agents in the immediate neighborhood, while movement of the first agent (the 'leader') is independent of the rest of the group (flock). For a given size of the flock, and the equilibrium (or 'desired') distances between the agents, it is found that there is a resonance frequency at which oscillatory movement of the leader produces large oscillations in the movement of all the other agents. In a more realistic situation, a sudden change in the movement of the leader produces an oscillatory effect on the rest of the flock, which dies out over time. We concentrate on finite size flocks, and derive second order approximation expressions for the resonance amplitude and frequency, which turn out to be quite precise for realistic flock sizes. We also perform extensive numerical simulations which illustrate the effect of the observed phenomenon on collective flock behavior for different choices for the leader motion.

We emphasize that here we study linearized equations without delay built in. While this is not likely to be the case in any natural (or technological) environment, these equations can nonetheless be considered as first order approximations of the

'real' equations. Thus to an extent, the phenomena here described do occur in Nature.

2. **Independent Leaders and Stability.** In this Section we introduce the notation and set up the equations for the two models we study analytically. Further details can be found in [3].

Let us suppose that the flock is traveling along the line and that the agents have positions x_i in the real line where $i \in \{0, \cdots N+1\}$. We will take the point of view that these positions represent cars on a one-lane road. Driver i adjusts his acceleration according to a pre-programmed algorithm considering the positions and velocities of his 'neighbors', that is: the cars he keeps track off. Who exactly these neighbors are depends on the example. Clearly, we wish to insure that for all $i \in \{1, \cdots N\}$, $x_{i-1} < x_i < x_{i+1}$ (the cars will collide if this condition is not satisfied). The zeroth car (or 'leader'), however, does not pay attention to the cars behind it (no-one is in front) and simply accelerates or decelerates according, for example, to the traffic lights the lead car encounters.

To get a feel for this kind of scenario we simplify even further. We assume that car number zero is executing a sine wave $a_0 \cdot \cos \omega t$, imposed on it from outside. This is referred to in [3] as "independent leader". The constant a_0 won't matter since after all we are dealing with linear equations, so we drop it. In the following the constant position and zero velocity vector $h \equiv (h_{x,0}, 0, h_{x,1}, 0, \cdots h_{x,N+1}, 0)^T$ encodes the desired position of the agents, and f and g are constants.

Let us first suppose that every car keeps track only of the car in front of it. With these considerations, the complexified linear equations of motion (together with the initial conditions) become:

$$\begin{aligned} \forall i \in \{1, \cdots, N+1\} \; : \; \dot{x}_i &= u_i \\ \dot{u}_i &= f\Big\{(x_i - h_{x,i}) - (x_{i-1} - h_{x,i-1})\Big\} + g\Big\{u_i - u_{i-1}\Big\} \\ \text{and} \qquad x_0 - h_{x,0} &= e^{i\omega t} \end{aligned} \tag{1}$$

where f and g are real constant. Our goal is to determine the real solutions of this system of differential equations (which represent the positions of the agents in the real line), however, in order to understand the dynamics of these equations, in what follows we consider their generalization to the complex plane, and treat x_i's as complex variables.

As a second example we shall consider the case where every car 'sees' the car in front and the one directly behind. This leaves us with one more "terminal" condition: car number $N+1$ sees only its predecessor, since there is no one following it. Such a situation may be of interest e.g. for automated vehicle design, or biological studies involving stability of large flocks, herds or schools. Under these assumptions, the complexified equations of motions (together with the initial conditions) become:

$$\begin{aligned} \forall i \in \{1, \cdots N\} \; : \; \dot{x}_i &= u_i \\ \dot{u}_i &= f\left\{(x_i - h_{x,i}) - \frac{1}{2}(x_{i-1} - h_{x,i-1} + x_{i+1} - h_{x,i+1})\right\} \\ &+ g\left\{u_i - \frac{1}{2}(u_{i-1} + u_{i+1})\right\} \\ \dot{x}_{N+1} &= u_{N+1} \\ \dot{u}_{N+1} &= f\Big\{(x_{N+1} - h_{x,N+1}) - (x_N - h_{x,N})\Big\} + g\Big\{u_{N+1} - u_N\Big\} \\ \text{and} \qquad x_0 - h_{x,0} &= e^{i\omega t} \end{aligned} \tag{2}$$

Following [3], Section 6, we introduce $x \equiv (x_1, u_1, x_2, u_2, \cdots, x_{N+1}, u_{N+1})^T$. Now let $\zeta \equiv (\zeta_1, 0, \zeta_2, 0, \cdots, \zeta_{N+1}, 0)^T$ be the vector encoding the desired relative positions of each agent with respect to the other. We can then write these equations of motion ((1) and (2)) with a single independent leader (denoted by the subscript 'ℓ') more succinctly in vector form as:

$$\dot{x} = I_{N+1} \otimes Ax + P_i \otimes K(x - \zeta) + L_\ell \otimes (K(x_\ell(t) - \zeta_\ell)) \quad ,$$

where I_{N+1}, L_i and P_i are the $(N+1)$-dimensional identity, Directed Laplacian, and Reduced Directed Laplacian, respectively (i equals 1 for in the first example and 2 in the second). Explicitly, in the first example

$$L_1 = \begin{pmatrix} 0 & 0 & 0 & 0\cdots \\ -1 & 1 & 0 & 0\cdots \\ 0 & -1 & 1 & 0\cdots \\ \vdots & & & \end{pmatrix} \quad \text{and} \quad P_1 = \begin{pmatrix} 1 & 0 & 0 & 0\cdots \\ -1 & 1 & 0 & 0\cdots \\ 0 & -1 & 1 & 0\cdots \\ \vdots & & & \end{pmatrix} \quad ,$$

and in the second example

$$L_2 = \begin{pmatrix} 0 & 0 & 0 & 0 & \cdots & \cdots \\ -1/2 & 1 & -1/2 & 0 & \cdots & \cdots \\ 0 & -1/2 & 1 & -1/2 & \cdots & \cdots \\ \vdots & & & & & \\ \cdots & \cdots & \cdots & 0 & -1 & 1 \end{pmatrix}$$

and

$$P_2 = \begin{pmatrix} 1 & -1/2 & 0 & 0 & \cdots & \cdots \\ -1/2 & 1 & -1/2 & 0 & \cdots & \cdots \\ 0 & -1/2 & 1 & -1/2 & \cdots & \cdots \\ \vdots & & & & & \\ \cdots & \cdots & \cdots & 0 & -1 & 1 \end{pmatrix} \quad ;$$

In both cases we have the constant matrices:

$$A \equiv \begin{pmatrix} 0 & 1 \\ 0 & 0 \end{pmatrix} \quad \text{and} \quad K \equiv \begin{pmatrix} 0 & 0 \\ f & g \end{pmatrix} \quad .$$

Thus $I \otimes A$ encodes the 'geodesic' part of the equations, K contains control parameters, $P \otimes K$ encodes the interaction of the cars with the appropriate neighbors and L_ℓ takes care of their interaction with the independent leader. The $N+1$-vector L_ℓ is given by the entries 1 through $N+1$ of the first column of L_i in each of the two examples. For the details of the notation and for the vector L_ℓ, see the cited paper. It turns out that $z = x - h$ we obtain the simple linear equation:

$$\dot{z} = (I_{N+1} \otimes A + P_i \otimes K)z + \Gamma(t) \ := M_i z + \Gamma(t) \quad , \tag{3}$$

where $\Gamma(t)$ represents the non-autonomous part of linear equations (1) and (2). Since $z = 0$ is an in formation solution, the eigenvalues of M_i determine whether in formation motion is stable.

We first want to insure that the formation is stable, so that the cars effectively have a tendency to travel together. This means that the eigenvalues of M must have negative real part. According to [1, 3, 4]:

$$\begin{aligned} \text{spec } (M)\backslash\{0\} &= \bigcup_{\lambda\in \text{ spec } (L_i)\backslash\{0\}} \{ \text{ spec } (A+\lambda K)\} \\ &= \bigcup_{\lambda\in \text{ spec } (L_i)\backslash\{0\}} \left\{ \text{spec } \begin{pmatrix} 0 & 1 \\ \lambda f & \lambda g \end{pmatrix} \right\} \quad . \end{aligned}$$

Now the spectrum of $L_i\backslash\{0\}$ equals that of P_i. The spectrum of P_1 equals $\{1\}$ with multiplicity $N+1$. One can also verify that the spectrum of the matrix P_2 is given by

$$\bigcup_{k\in\{1,\cdots N+1\}} \left\{ 1-\cos\left(\frac{2k-1}{2(N+1)}\,\pi\right)\right\}$$

all simple real eigenvalues (the spectrum of this kind of matrices can be solved using the Rayleigh-Ritz method [5]). In turn, the eigenvalues of the matrix $A+\lambda K$ are given by the solutions of:

$$x^2-\lambda g x-\lambda f=0 \quad \Longrightarrow \quad x_\pm=\frac{1}{2}\left(\lambda g\pm\sqrt{(\lambda g)^2+4\lambda f}\right) \quad .$$

Putting together these facts, one easily concludes that:

Lemma 1. *Both systems are* uniformly *(in N) stabilized if and only if both f and g are strictly smaller than zero.*

Remark: Here as well as in the cited papers we assume that f and g are real parameters. The possibility that they may be complex parameters is to the best of our knowledge unexplored at the date of this writing.

Thus choosing both f and g constant and negative, the eigenvalues of M_i all have negative real part (the zero eigenvalue has effectively been removed from the system which does not contain a differential equation for the 'leader'). Thus the system will tend to its *particular* solution. The full details of the graph theoretical aspect of this discussion can be found in [2].

3. **Tracking only the agent in front.** In this Section we shall demonstrate that it is a rather bad idea to keep track only of the agent immediately in front. To this end, we explore the behavior of the last agent when the position the leader performs harmonic oscillations.

The current problem is a represented by system of first order linear differential equations with periodic forcing. The general solution of such a system is the sum of the homogeneous solutions plus the particular solution. We know (Lemma 1) that the homogeneous solutions decay to zero because the real part of the spectrum is negative, therefore we focus on finding the particular solution of equation (1). In this case there is a particular solution of the form $x_k=a_k e^{i\omega t}$, where the real part of x_k represents solutions that have physical or biological sense.

Remark: For completeness it should be mentioned here that if each agent keeps track of only the one directly behind, things will definitely go very wrong, since in that case no-one sees the leader.

Corollary 1. *If we only track the agent in front, then* $a_k = \gamma^{-k}$ *where* $\gamma \equiv \dfrac{f + i\omega g + \omega^2}{f + i\omega g}$. *In particular, if we set* $\omega^2 = |f|$, *then the particular solution is determined by* $x_k = a_k e^{i\omega t}$ *where* $a_k = \left(1 + i\dfrac{\sqrt{|f|}}{g}\right)^k$.

Proof: All we have to do to complete the calculations is to analyze the particular solution of the system. We do this by substituting $x_k = a_k e^{i\omega t}$ and $u_k = i\omega e^{i\omega t}$ in Equation (1). We immediately obtain

$$-\omega^2 a_k = f(a_k - a_{k-1}) + i\omega g(a_k - a_{k-1}) \quad .$$

This leads to the following recurrence equation

$$a_k = \frac{f + i\omega g}{f + i\omega g + \omega^2}\, a_{k-1} \quad .$$

We will use the shorthand γ^{-1} for the fraction in the last expression. It follows that the particular solution is given by:

$$a_k = \gamma^{-k} a_0 \quad .$$

It is easy to see that $|\gamma^{-1}|$ is greater than one if and only if $\omega^2 < 2|f|$ (recall that f and g are less than zero). The spatial instability is strongest when

$$\omega^2 = |f| \quad \Longrightarrow \quad a_k = \left(1 + i\frac{\sqrt{|f|}}{g}\right)^k a_0 \quad .$$

□

Remark: If we assume that $h_{k+1} - h_k = 1$, the separation between two successive agents is given by

$$a_0 \mathrm{Re}\left(\gamma^{-k-1} e^{i\omega t}\right) - a_0 \mathrm{Re}\left(\gamma^{-k} e^{i\omega t} + 1\right)$$

Proposition 1. *If the amplitude of the oscillation of the leader at frequency* $|f|$ *is* a_0, *and the maximum oscillation allowed is* D, *then of course, the size of the flock is limited by:*

$$N \lesssim 2\, \frac{\ln(D/a_0)}{\ln(1 + |f|/g^2)} \quad .$$

Note that not only is there a spatial instability, but there is also a constant phase lag between two successive agents given by the angle of γ.

4. **Tracking the two agents in the immediate front and back.** This case has more potential for real applications, but is somewhat harder to analyze. We use the notation of the previous section, and in addition the square root with angle in $(-\pi/2, \pi/2]$ of a complex number z is indicated with $\sqrt{z}$, γ is as defined in the previous section, and $C \equiv \begin{pmatrix} 0 & 1 \\ -1 & 2\gamma \end{pmatrix}$.

Lemma 2. *In the case where only the agents immediately preceding and the trailing each agent are tracked, we have*

$$a_{N+1}(f, g, \omega) = \frac{2}{\mathrm{Tr}\, C^{N+1}} = \frac{2}{\mu_-^{N+1} + \mu_+^{N+1}} \quad .$$

Proof: We follow the same strategy as before (finding the particular solution) and substitute $x_k = a_k e^{i\omega t}$ and $u_k = i\omega a_k e^{i\omega t}$ in Equation (2). We immediately obtain

$$-\omega^2 a_k = f\left(a_k - \frac{1}{2}(a_{k+1} + a_{k-1})\right) + i\omega g\left(a_k - \frac{1}{2}(a_{k+1} + a_{k-1})\right) \quad .$$

This system is equivalent to:

$$\begin{pmatrix} a_k \\ a_{k+1} \end{pmatrix} = \begin{pmatrix} 0 & 1 \\ -1 & 2\gamma \end{pmatrix} \begin{pmatrix} a_{k-1} \\ a_k \end{pmatrix} \quad .$$

Recall that γ was defined is Section 3. The matrix will be denoted by C. This is a second order system, and is subject to two 'boundary' conditions, namely:

$$a_0 = 1 \qquad \text{and} \qquad a_{N+1} = \gamma^{-1} a_N \quad .$$

The second equation comes about because the last agent can only see the car in front of it.

Define

$$\mu_\pm \equiv \gamma \pm \sqrt{\gamma^2 - 1} \quad , \tag{4}$$

then C has the following eigenvectors:

$$v_- = \begin{pmatrix} 1 \\ \mu_- \end{pmatrix} \text{ with eigenvalue } \mu_- \text{ and } v_+ = \begin{pmatrix} 1 \\ \mu_+ \end{pmatrix} \text{ with eigenvalue } \mu_+.$$

Thus, in view of the first boundary condition:

$$\begin{pmatrix} a_0 \\ a_1 \end{pmatrix} = c_+ \begin{pmatrix} 1 \\ \mu_+ \end{pmatrix} + (1 - c_+) \begin{pmatrix} 1 \\ \mu_- \end{pmatrix} \quad .$$

The constant c_+ can be determined by requiring that $C^N \begin{pmatrix} a_0 \\ a_1 \end{pmatrix}$ satisfy the second boundary condition.

$$C^N \begin{pmatrix} a_0 \\ a_1 \end{pmatrix} = \begin{pmatrix} c_+\mu_+^N + (1 - c_+)\mu_-^N \\ c_+\mu_+^{N+1} + (1 - c_+)\mu_-^{N+1} \end{pmatrix} = \begin{pmatrix} \gamma a_{N+1} \\ a_{N+1} \end{pmatrix}$$

Using that $(1 - \gamma\mu_\pm) = (\sqrt{\gamma^2 - 1})\mu_\pm$, we solve for c_+ to get:

$$c_+ = \frac{(1 - \gamma\mu_-)\mu_-^N}{(1 - \gamma\mu_-)\mu_-^N - (1 - \gamma\ \mu_+)\mu_+^N} = \frac{\mu_-^{N+1}}{\mu_-^{N+1} + \mu_+^{N+1}} \quad .$$

Substituting this back into the second component of $C^N \begin{pmatrix} a_0 \\ a_1 \end{pmatrix}$ and using that $\mu_-\mu_+ = 1$ gives the desired relation. □

Corollary 2. *For $\omega \neq 0$, we have that $|\mu_+| \neq |\mu_-|$ and thus for fixed ω, a_N decays exponentially (as function of the size N of the flock). (For low frequencies this decay may be slow.)*

Proof: The product of the eigenvalues $\mu_\pm$ equals 1. So it suffices to show that the modulus of μ_+ is not equal to 1 if $\omega \neq 0$. In view of Equation (4) we need to solve:

$$\mu_+ = \gamma + \sqrt{\gamma^2 - 1} = e^{i\phi} \quad ,$$

where ϕ is a real number. This implies that $\gamma = \cos\phi$. However, it is also easy to check from the definition of γ that γ is real-valued if and only if $\omega = 0$. In turn this is equivalent with $\mu_+ = \mu_-$. □

We illustrate these ideas by picturing $\ln|a_N(f,g,\omega)|$ for $N=100$ and $N=1000$ in Figures 1. In these pictures both f and g are held fixed at -1. As stated before, we are really interested in *finite size* effects, and much less in the limit as $N\to\infty$. It is natural to study a_N for fixed N as function of ω. These pictures predict that the response for a flock of 100 individuals peaks at about $\omega=0.011$ and those of 1000 individuals at a frequency 10 times less. The height of the maximum peak determines the amplitude of the response. In order to understand this we need to analyze the expression given in the Lemma.

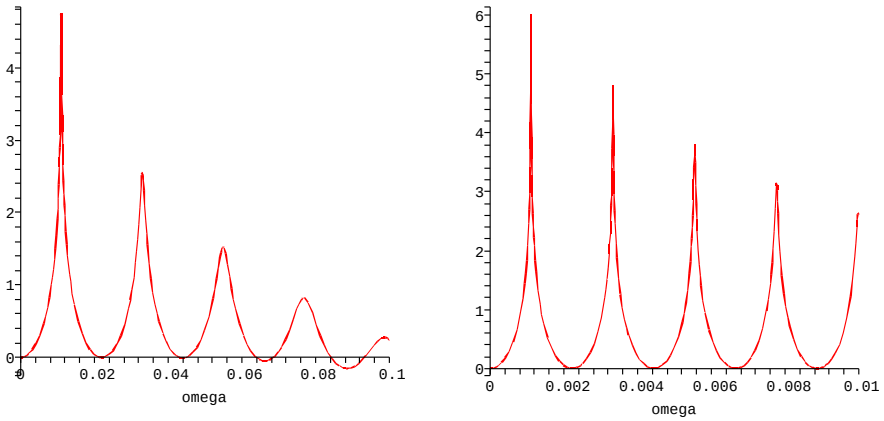

FIGURE 1. *Picture of* $\ln|a_{100}(f=-1,g=-1,\omega)|$ *and of* $\ln|a_{1000}(f=-1,g=-1,\omega)|$ *(varying* ω*).*

5. **The Finite Size Resonance.** We derive the location and size of the resonance up to *two* orders (in N^{-1}) of approximation (Theorem 1).

As observed in the previous section, this resonance is due to the fact that the flock is finite and large. It is caused by small divisor issues in the expression for a_N given in Lemma 2. As is clear from that Lemma and the fact that the product of μ_+ and μ_- equals 1, the only a_N gets big is if cancellation in the denominator occurs. For this to happen μ_+ and μ_- must both tend to 1, and this of course happens if and only if ω tends to zero. Thus we have:

Lemma 3. *A necessary condition (if* ω *is real) for a resonance in the system of Section 4 is that* $|\omega|$ *is small.*

Theorem 1. *For large flocks the main resonance is located at*

$$\omega=\frac{\sqrt{|f|}\pi}{(N+1)2\sqrt{2}}+\mathcal{O}(N^{-3})\quad,$$

and its peak size is given by

$$A=\frac{8\sqrt{2|f|}}{\pi^2|g|}\,(N+1)+\mathcal{O}(N^{-1})\quad.$$

Proof: From Lemma 2 one concludes that the only way a resonance can occur is when the divisor of the formula for a_N becomes small, which may happen when both eigenvalues are close to 1 (or equivalently γ is close to 1, or $|\omega|$ is small), so in what follows this condition will be assumed.

We go back to Lemma 2. For a resonance we need that $\mu_+^{N+1} + \mu_-^{N+1}$ is close to zero. Denoting $\sqrt{\gamma^2 - 1}$ by ϵ and assuming that ω is positive, we see that

$$\gamma - 1 = \frac{\epsilon^2}{2 + (\gamma - 1)} \quad .$$

Thus $\gamma - 1 = \mathcal{O}(\epsilon^2)$ and we obtain

$$\mu_\pm = \gamma \pm \epsilon = 1 \pm \epsilon + \frac{\epsilon^2}{2} + \mathcal{O}(\epsilon^4) \quad .$$

We first calculate ϵ in terms of ω.

$$\begin{aligned} \epsilon &= \sqrt{\left(1 + \frac{\omega^2}{f^2 + \omega^2 g^2}(f - i\omega g)\right)^2 - 1} \\ &= \sqrt{\frac{2\omega^2}{f^2}(f - i\omega g)\left(1 + \frac{\omega^2 g^2}{f^2}\right)^{-1} + \frac{\omega^4}{f^4}(f - i\omega g)^2\left(1 + \frac{\omega^2 g^2}{f^2}\right)^{-2}} \quad , \end{aligned}$$

thus, taking into account that f and g must be negative (by Lemma 1), we find

$$\begin{aligned} \epsilon &= i\sqrt{2}\frac{\omega}{\sqrt{|f|}}\sqrt{\left(1 - \frac{i\omega|g|}{|f|}\right)\left(1 + \frac{\omega^2 g^2}{f^2}\right)^{-1} - \frac{\omega^2}{2|f|}\left(1 - \frac{i\omega|g|}{|f|}\right)^2\left(1 + \frac{\omega^2 g^2}{f^2}\right)^{-2}} \\ &= i\sqrt{2}\frac{\omega}{\sqrt{|f|}}\left(\left(1 - \frac{i\omega|g|}{2|f|}\right) + \frac{\omega^2}{2}\left(-\frac{g^2}{f^2} - \frac{1}{2|f|}\right)\right) + \mathcal{O}(\omega^4) \quad . \end{aligned}$$

From this it follows that for small ω, $\mathcal{O}(\epsilon^n)$ can be replaced by $\mathcal{O}(\omega^n)$. Next we substitute the above expression into the one for $\mu_\pm$, and after some manipulation we obtain

$$\mu_\pm = 1 - \frac{\omega^2}{|f|} \pm \frac{\omega^2|g|}{\sqrt{2}|f|^{3/2}} + i\left(\pm\frac{\sqrt{2}\omega}{|f|^{1/2}} \pm \mathcal{O}(\omega^3)\right) + \mathcal{O}(\omega^4) \quad .$$

From this we calculate

$$\tan(\angle\mu_\pm) = \frac{\pm\frac{\sqrt{2}\omega}{|f|^{1/2}} + \mathcal{O}(\omega^3)}{1 - \frac{\omega^2}{|f|} \mp \frac{\omega^2|g|}{\sqrt{2}|f|^{3/2}} + \mathcal{O}(\omega^4)} \qquad \text{or} \qquad \angle\mu_\pm = \pm\sqrt{2}\frac{\omega}{\sqrt{|f|}} + \mathcal{O}(\omega^3) \quad ,$$

and

$$|\mu_\pm|^2 = \left(1 + \frac{\omega^2}{|f|}\left(-1 \pm \frac{|g|}{\sqrt{2}|f|^{1/2}}\right)\right)^2 + \frac{2\omega^2}{|f|} + \mathcal{O}(\omega^4) = 1 \pm \sqrt{2}\omega^2\frac{|g|}{|f|} + \mathcal{O}(\omega^4) \quad .$$

This puts us finally in a position where we can prove both statements of the theorem. When the system is in resonance, the angles of $\mu_\pm^{N+1}$ must be equal and opposite in sign and their moduli must be approximately equal. The smallest value of ω for which this can happen is when $\mu_\pm^{N+1}$ is approximately equal to $\pm i$. The smallest value for ω means that $|\mu_\pm|$ are close to one, and thus the denominator in

Lemma 2 is smallest, making this resonance the principal one. We thus have that when the system is in (principal) resonance

$$\angle \mu_{\pm}^{N+1} = (N+1)\left(\frac{\sqrt{2}\omega}{|f|^{1/2}} + \mathcal{O}(\omega^3)\right) = \frac{\pi}{2} \quad .$$

This clearly implies that (when the system is in resonance at some small omega) we may replace $\mathcal{O}(\omega^n)$ by $\mathcal{O}(N^{-n})$. By using that and solving for ω we obtain the first statement.

Next we need to calculate $|\mu_-^{N+1} + \mu_+^{N+1}|$ when the system is in principal resonance (that is: using the first statement of the theorem). At resonance this is equal to $|\mu_+|^{N+1} - |\mu_-|^{N+1}$.

$$\begin{aligned} |\mu_\pm|^{N+1} &= \left[1 \pm \frac{\sqrt{2}\omega^2|g|}{|f|^{\frac{3}{2}}} + \mathcal{O}(\omega^4)\right]^{\frac{N+1}{2}} = \left[1 \pm \frac{\sqrt{2}\omega^2|g|}{|f|^{\frac{3}{2}}}\right]^{\frac{N+1}{2}} + \mathcal{O}(N^{-3}) \\ &= \left[1 \pm \frac{\pi^2|g|}{4\sqrt{2|f|}(N+1)^2}\right]^{\frac{N+1}{2}} + \mathcal{O}(N^{-3}) \quad . \end{aligned}$$

To simplify notation a bit, let $x \equiv \frac{\pi^2|g|}{8\sqrt{2|f|}}$. We now use the series expansions of $\sqrt{1 \pm 2x}$ and of e^x.

$$\begin{aligned} |\mu_\pm|^{N+1} &= \left(1 + \frac{\pm 2x}{(N+1)^2}\right)^{\frac{N+1}{2}} + \mathcal{O}(N^{-3}) = \left(1 + \frac{\pm x}{(N+1)^2}\right)^{N+1} + \mathcal{O}(N^{-3}) \\ &= \sum_{k=0}^{N+1} \binom{N+1}{k} \left(\frac{\pm x}{(N+1)^2}\right)^k + \mathcal{O}(N^{-3}) \\ &= \sum_{k=0}^{N+1} \frac{1}{k!} \left(\frac{\pm x}{N+1}\right)^k + \mathcal{O}(N^{-3}) = e^{\frac{\pm x}{N+1}} + \mathcal{O}(N^{-3}) \quad . \end{aligned}$$

And thus we finally obtain:

$$|\mu_+|^{N+1} - |\mu_+|^{N+1} = \frac{2x}{N+1} + \mathcal{O}(N^{-3}) \quad \Longrightarrow \quad A \equiv |a_{N+1}| = \frac{N+1}{x} + \mathcal{O}(N^{-1}) \quad .$$

Substituting the expression for x into this, gives the second estimate. □

From these calculations, we can in fact deduce something slightly more.

Corollary 3. *There are lesser resonances located roughly at the odd multiples of the main resonance.*

Proof: Left to the reader. It follows from the considerations in the previous proof. □

Proposition 2. *If the amplitude of the oscillation at the frequency of the principal resonance of the leader is a_0, and the maximum oscillation allowed is D, then the size of the flock is limited by:*

$$N \lesssim \frac{\pi^2|g|}{8\sqrt{2}\sqrt{|f|}} \frac{D}{a_0} \quad .$$

Remark: Note the difference with Proposition 1. Here the maximum size is *linear* in D/a_0.

6. **Stop and Go Traffic Led by a Single agent.** We apply these ideas to a thought experiment, where we imagine a sequence of 1-dimensional agents. They are all on 'automatic pilot' according to the algorithm given by Equation (2). The leader accelerates abruptly with non-zero, constant acceleration when the traffic light in front of it turns green. As soon as it reaches the target velocity, its acceleration abruptly drops to zero. The agents trailing it are supposed to follow safely (without collisions and with a minimum in fluctuations of their velocities).

It is clear that we will see some oscillatory behavior near, or at, the resonance frequency (see Figure 5), and this is born out by numerical tests. While naively one would expect that the amplitude of the oscillation will be easily predicted as well, this turns out not to be the case. In particular the dependence on the parameter g seems weak at best. The calculation of the maximum amplitude of this 'traffic-like' oscillation appears a slightly more subtle problem than simply calculating the resonant amplitude and we will discuss this in a separate work.

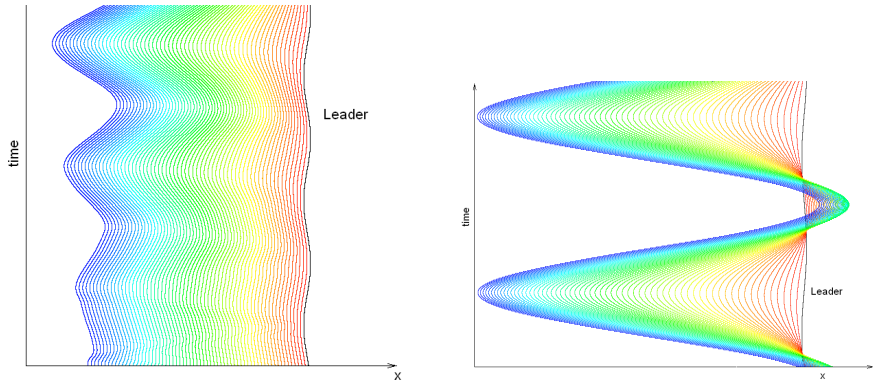

FIGURE 2. Flock behavior for periodic leader movement at resonance frequency, starting from equidistant positions and zero velocities a) at an early stage and b) close to equilibrium.

There are several reasons for this problem. First the position $x_0(t)$ of the leader is not an integrable function. So any naive Fourier analysis of that signal runs afoul of the fact that the integrals involved do not converge. The second reason can be guessed from the first two figures in this section. By linearity all modes are independent. In physical terms, the oscillatory behavior of the leader at the resonant frequency can inject its energy only very slowly into the system (because the flock members acquire much larger amplitude than the leader). Thus it takes some time for the last members of the system to get close to achieving their equilibrium resonance. In Figures 2 a) and b), we display the flock behavior for periodic leader movement at resonance frequency at the very beginning of the process (starting from equidistant flock member positions and zero velocities), and close to equilibrium (maximum amplitudes), respectively. However, in the mean time the global stability of the system has been driving the system back to coherent movement. Thus the amplitude of the oscillation never reaches its full 'resonant' size.

Several remarks are in order. If each agent keeps track of only the n-th agent in front and behind it, the communication graph is not connected and therefore some agents will stay behind.

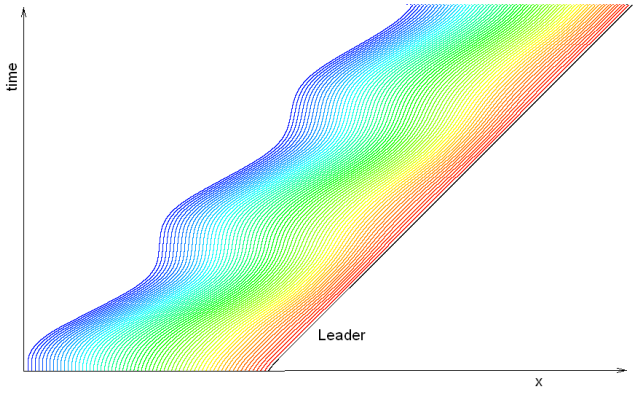

FIGURE 3. *Flock behavior for discontinuous leader acceleration.*

More interesting is the question for which kind of connected communication graphs this finite resonance plays a role and for which kind of graphs the spatial amplification of a perturbation is exponential. Numerous experiments that we have performed with more complicated communication graphs of agents on a line, indicate that these are the only two possibilities. However, how to distinguish these graphs from one another is not clear yet. It appears that to be able to sense to the same numbers of agents in front as behind is an important (though not decisive) factor. Again this is the subject of future study.

7. **Numerical Methods and Experiments.** In this section we compare the asymptotic estimate of the main resonance for large flocks with numerical experiments. The experiments reported on in detail in this section all concern the system given by Equation (1). The behavior of the system given by Equation (2) is relatively simple and is discussed in Section 3.

The differential equations given in (1) were computed for a set of values of N, the initial conditions were fixed such that every agent started from its equilibrium position. The numerical integration was done until the solution reached its stable state. The peak size of the oscillation of the last agent is compared with the asymptotic estimation obtained in Theorem 1, this results are shown in the accompanying table.

Numerical integration of the system of coupled equations given in (2) is complicated by the fact that acceleration of a given flock member depends on position and velocity of the neighboring members, so that integrators that require ability to calculate the derivatives, such as Runge-Kutta and Bulirsch-Stoer method, cannot be applied in their usual form: one cannot calculate the derivatives at arbitrary moments of time. We succeeded in implementing both fourth order Runge-Kutta and a simplified version of the Bulirsch-Stoer algorithm with polynomial extrapolation by implementing virtual steps of varying size. Nonetheless it turns out that the precision gain, obtained by making "better" steps, is countered by the task of calculating the virtual steps, in particular when the system is still far from equilibrium. We find that the best precision/time ratio is obtained by combining the

N	NFREQ	NAMP	TFREQ	TAMP
4	0.2776801836	4.58527335	0.2727291	4.49064609
8	0.1388400918	9.17054669	0.1382221	9.11739657
16	0.0694200459	18.34109338	0.06934994	18.3135253
32	0.0347100229	36.68218677	0.03470038	36.6683866
64	0.0173550115	73.36437354	0.017353935	73.3562112
128	0.0086775057	146.72874707	0.008677381	146.7227220

Table 1: Values of resonance amplitude and frequency of the last member of the flock of size $N+2$ (including leader), obtained through numerical simulations (columns NFREQ and NAMP) , together with the corresponding second order approximation values (columns TFREQ and TAMP).

elementary Euler method for flock configurations far from equilibrium, with a higher order method close to equilibrium. To achieve better performance, we also apply adaptive step size and adaptive error requirements (decreasing steps and increasing precision as equilibrium is approached). With this technique we obtained results for flock sizes up to $N = 128$, in several hours CPU time, on a 3GHz Pentium machine with a dedicated C program.

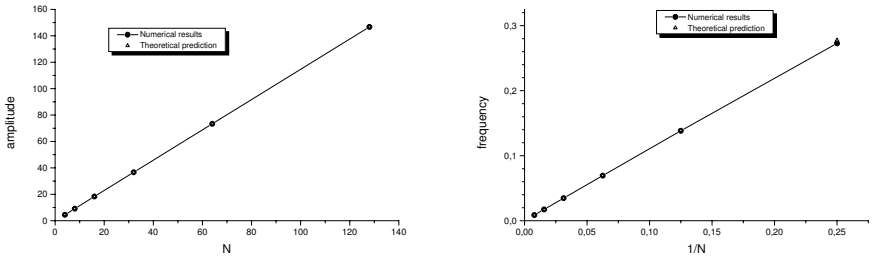

FIGURE 4. *Values of resonance a) amplitude and b) frequency of the last flock member as a function of flock size, obtained through numerical simulations, together with the corresponding second order approximation values.*

Simulations were performed with $f = g = -1$, starting from equilibrium position $x_i = -i$, where $i = 1, \cdots N+1$, with the leader (at $x = 0$) oscillating at different frequencies (this includes the simulations in the previous section), with the leader's amplitude $a_0 = 1$. For each system size, we begin simulations at the second order approximation for the resonant frequency $\omega_0 = \pi\sqrt{2}/4(N+1)$, given by Theorem 1, and iterate the system until amplitude stabilizes with relative precision of $\epsilon = 10^{-8}$. Next, we repeat the same procedure below and above the second order approximation (given by the same Theorem) in order to bracket the amplitude maximum, and then we proceed to find the maximum implementing the golden section search.

Results of our numerical simulations are summarized in Table 1, where we display the numerical values of frequency and amplitude (where we show only the relevant

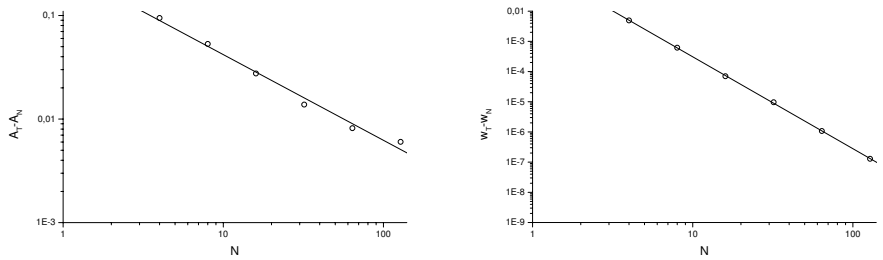

FIGURE 5. *Difference between the resonance a) amplitude and b) frequency obtained through numerical simulations and the corresponding second order approximation, as a function of flock size.*

digits), and the corresponding second order approximation values. In Figure 4 we display the comparison of numerical results and the second order approximation for amplitude and frequency, where it is seen that the agreement is excellent. Furthermore, in Figure 5 we show the difference between the numerical and second order approximation frequency values as a function of flock size, on the logarithmic scale, together with the regression line (least squares). The slope of the regression line close to -3 indicates that second order prediction is indeed correct.

Acknowledgements. JJPV gratefully acknowledges a fellowship granted by the Spanish Government through its Ministry of Science and Education enabling him to dedicate an academic year to research while based in Granada, Spain.

REFERENCES

[1] J. S. Caughman, G. Lafferriere, J. J. P. Veerman and A. Williams, *Decentralized Control of Vehicle Formations*, Systems & Control Letters, **54** (2005), 899–910.
[2] J. S. Caughman and J. J. P. Veerman, *Kernels of Directed Graph Laplacians*, Electr. J. Comb. 13, **1** (2006).
[3] J. J. P. Veerman, John S. Caughman, G. Lafferriere and A. Williams, *Flocks and Formations*, J. Stat.Phys. **121** (2005), 901–936.
[4] A. Williams, G. Lafferriere and J. J. P. Veerman, *Stable Motions of Vehicle Formations*, in "Proc. 44th Conference of Decision and Control", (2005), 72–77.
[5] G. H. Golub and C. F. Van Loan "Matrix Computation," North Oxford Academic, Oxford, 1983.

Received April, 2007; revised August 2007.

E-mail address: veerman@pdx.edu
E-mail address: borko@ufpe.br
E-mail address: aoc@mym.iimas.unam.mx